Quantum quench dynamics and population inversion in bilayer graphene

Balázs Dóra,[1,2,*] Eduardo V. Castro,[3,4] and Roderich Moessner[1]
[1]*Max-Planck-Institut für Physik komplexer Systeme, Nöthnitzer Str. 38, 01187 Dresden, Germany*
[2]*Department of Physics, Budapest University of Technology and Economics, Budafoki út 8, 1111 Budapest, Hungary*
[3]*Instituto de Ciencia de Materiales de Madrid, CSIC, Cantoblanco, E-28049 Madrid, Spain*
[4]*Centro de Física do Porto, Rua do Campo Alegre 687, P-4169-007 Porto, Portugal*
(Received 23 August 2010; published 23 September 2010)

The gap in bilayer graphene (BLG) can directly be controlled by a perpendicular electric field. By tuning the field through zero at a finite rate in neutral BLG, excited states are produced. Due to screening, the resulting dynamics is determined by coupled nonlinear Landau-Zener models. The generated defect density agrees with Kibble-Zurek theory in the presence of subleading logarithmic corrections. After the quench, population inversion occurs for wave vectors close to the Dirac point. This could, at least, in principle, provide a coherent source of infrared radiation with tunable spectral properties (frequency and broadening). Cold atoms with quadratic band crossing exhibit the same dynamics.

DOI: 10.1103/PhysRevB.82.125441 PACS number(s): 81.05.ue, 64.60.Ht, 78.67.Wj

I. INTRODUCTION

Charge carriers in bilayer graphene (BLG), which consists of two atomic layers of crystalline carbon, combine nonrelativistic "Schrödinger" (quadratic dispersion) and relativistic "Dirac" (chiral symmetry, unusual Berry phase) features. Due to their peculiar nature, BLG holds the promise of revolutionizing electronics since its band gap is directly controllable by a perpendicular electric field over a wide range of parameters[1–5] (up to 250 meV (Ref. 6)], unlike existing semiconductor technology. Moreover, unlike monolayer graphene (MLG), whose effective model (the Dirac equation) was thoroughly studied in QED and relativistic quantum mechanics, understanding the low-energy properties of BLG is a new challenge.

Tuning the gap through zero in BLG in a time-dependent perpendicular electric field parallels closely to a finite rate passage through a quantum critical point (QCP): as the gap closes, activated behavior and a finite correlation length give way to metallic response and power-law correlations, as in a sweep through a QCP. During the latter, defects (excited states and vortices) are produced according to Kibble-Zurek theory.[7,8] When the relaxation time of the system, which encodes how much time it needs to adjust to new thermodynamic conditions, becomes comparable to the remaining ramping time to the critical point, the system crosses over from the adiabatic to the diabatic (impulse) regime. In the latter regime, its state is effectively frozen so that it cannot follow the time dependence of the instantaneous ground states—as a result, excitations are produced.[9] Evolution restarts only after leaving the diabatic regime, with an initial state mimicking the frozen one. The theory, general as it is, finds application in very different contexts in physics, ranging from the early universe cosmological evolution[7] through liquid ^{3,4}He (Refs. 8, 10, and 11) and liquid crystals[12,13] to ultracold gases,[14] verified for both thermodynamic and quantum phase transitions.[15] The relative case of manipulating the gap—in particular, in real time—via a spatially uniform external electric field, which can therefore play the role of a (time-dependent) control parameter, establishes BLG as an ideal setting for the study of quantum quenches with sudden, continuous, or any other sweep protocols.[16–18] This in turn leads to the question: what might such states be useful for?

This complex of questions is addressed here. In particular, we compute the defect (excited state) density after a slow, nonadiabatic gap-closing passage in BLG via Kibble-Zurek[7,8] theory, taking screening between the layers into account. The presence of excited states after such a quench leads to population inversion for wave vectors near the Dirac point in BLG (see Fig. 1), evidenced by the dynamic conductivity. This could, in principle, provide a coherent source of infrared radiation with tunable spectral properties (frequency and broadening), determined below in an idealized model. This is promising as there are only few materials that generate light in the infrared with tunable frequency; BLG with its unique properties might represent the first step toward new lasers for this regime.

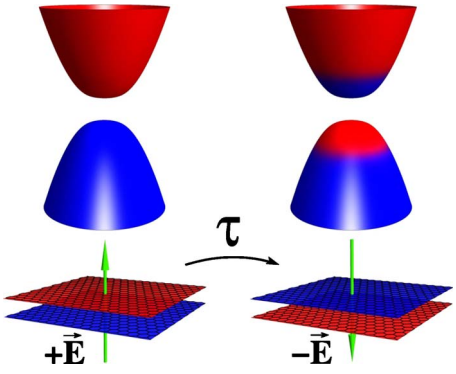

FIG. 1. (Color online) Reversing the applied perpendicular electric field $+\vec{E}$ in half-filled BLG (left) at a finite rate $1/\tau$ leads to excited states in the upper branch in accordance with the Kibble-Zurek theory of nonequilibrium phase transitions (right). The momentum distribution increases from red/bright (0) to blue/dark (1) in the spectra. Realistic quenching times provide an effective population inversion with little effect on the layer charge asymmetry.

 ©2010 The American Physical Society

II. HAMILTONIAN, TOPOLOGICAL PROPERTIES

We study the problem in a more general setting of a general class of low-energy Hamiltonians, comprising monolayer and bilayer graphene, which exhibit quantum critical behavior, as

$$H = \begin{pmatrix} \Delta & c_J(p_x - ip_y)^J \\ c_J(p_x + ip_y)^J & -\Delta \end{pmatrix}, \tag{1}$$

where J is a positive integer. The energy spectrum is given by $E_\pm(p) = \pm\sqrt{\Delta^2 + \varepsilon^2(p)}$ with $\varepsilon(p) = c_J|p|^J$ the gapless spectrum, $|p| = \sqrt{p_x^2 + p_y^2}$ with spatial dimension $d=2$.

The critical exponents can straightforwardly be read off. The correlation length follows from dimensional analysis: $\xi \sim \hbar(c_J/|\Delta|)^{1/J}$, defining $\nu = 1/J$. The Hamiltonian contains the Jth spatial derivative (Jth power of p), which leads to $z = J$. The resulting scaling relation $z\nu = 1$ is in agreement with a linearly vanishing gap Δ. To understand the nature of this criticality, let us take a closer topological look at Eq. (1) by evaluating the Berry curvature (Ω_p) for a given J, which is related to the phase picked up during an adiabatic excursion in the Brillouin zone as[19]

$$\Omega_p = \nabla_{\mathbf{p}} \times \mathbf{A}(\mathbf{p}) \tag{2}$$

with $\mathbf{A}(\mathbf{p}) = -i\langle n\mathbf{p}|\nabla_{\mathbf{p}}|n\mathbf{p}\rangle$, $|n\mathbf{p}\rangle$ is the eigenfunction in the nth band. For Eq. (1), we obtain for the z component of the Berry curvature per valley and spin,

$$\Omega_p^z = \frac{\Delta}{2E_+(p)}\left[\frac{d\varepsilon(p)}{d|p|}\right]^2 = \frac{\Delta J^2 c_J^2 |p|^{2(J-1)}}{2[\Delta^2 + \varepsilon^2(p)]^{3/2}}, \tag{3}$$

and its integral defines a topological invariant[20] as

$$\mathcal{C}_J = \frac{1}{2\pi}\int d^2p\,\Omega_p^z = \frac{J}{2}\mathrm{sign}(\Delta). \tag{4}$$

Therefore, the sign change in Δ corresponds to a change in the topological properties of Eq. (1). In addition, the Hall conductivity also exhibits a step as Δ passes through zero, and depends on the very same topological invariant per spin and valley as

$$\sigma_{xy} = \frac{e^2}{h}\mathcal{C}_J = \frac{e^2}{h}\frac{J}{2}\mathrm{sign}(\Delta). \tag{5}$$

States with different values of $\mathcal{C}_J$ can be regarded as belonging to distinct phases, similarly to the σ_{xy} plateau phases of the integer quantum-Hall effect.[21] Note, that low-energy Hamiltonians like Eq. (1) usually occur pairwise (i.e., at the K and K′ points in the Brillouin zone for graphene). Therefore, the topological invariants, $\mathcal{C}_J$ from different valleys, add up to integer (not necessarily zero) Chern numbers. A Δ from spin-orbit coupling can trigger a nonzero Chern number while the contribution from different valleys due to a staggered sublattice potential or bias voltage lead to a zero Chern number, although each valleys can have nontrivial topology with finite C_J. Spin degeneracy also leads to an additional factor of 2.

III. QUENCHING THE GAP

We are interested in the quantum quench dynamics when the gap varies as $\Delta(t) = \Delta_0 t/\tau$ (up to logarithmic corrections, as analyzed below) and $t \in [-\tau, \tau]$. According to Kibble-Zurek scaling,[7,8] the resulting defect (extra electron/hole on the hole/electron rich layer, respectively, equivalent to excited states in the upper branch in this case[22]) density is $\rho \sim \tau^{-d\nu/(z\nu+1)}$, which leads to

$$\rho \sim (\Delta_0/\tau)^{1/J}. \tag{6}$$

The matrix structure of Eq. (1) allows us to connect our problem to the Landau-Zener (LZ) dynamics[23] by analyzing the solution of

$$i\hbar\partial_t\Psi(t) = H\Psi(t), \quad \Psi(-\tau) = \Psi_-, \tag{7}$$

where $H\Psi_\pm = E_\pm\Psi_\pm$, and the quantity of interest is $\Psi(\tau)$. Considering finite temperatures amounts to change the initial condition as a combination of positive and negative energy states. However, as long as $k_BT \ll \Delta_0$, our results hold. The exact solution for the diabatic transition probability between final ground and excited states at momentum p for $\varepsilon(p) \ll \Delta_0$ gives for the momentum distribution of excited states in the upper branch (Fig. 1) and the resulting total defect density

$$P_p = \exp[-\pi\varepsilon^2(p)\tau/\hbar\Delta_0], \tag{8}$$

$$\rho = \frac{A_c}{(2\pi\hbar)^2}\int d^2p P_p = \frac{A_c\Gamma(1/J)}{4J\pi\hbar^2}\left(\frac{\hbar\Delta_0}{\pi c_J^2\tau}\right)^{1/J} \tag{9}$$

per valley, spin, and unit cell, with A_c the unit-cell area. This agrees with Kibble-Zurek scaling in Eq. (6). However, the present approach also provides the explicit numerical prefactor for arbitrary J, similarly to the quantum Ising model.[24] Note that the bigger J, the larger (and the more insensitive to τ) the resulting defect density, on account of the larger the number of low-energy states ($\omega^{2/J}$) within an energy window ω around the Dirac point.

Since the number of defects from Eq. (9) progressively increases with decreasing τ, it is important to address its validity. From Ref. 18, the borderline between a sudden and slow quench is determined from $\hbar d\Delta/dt \sim \Delta^2$, which yields $\tau\Delta_0 \sim \hbar$. Thus, our results apply in the slow quench regime when $\tau\Delta_0 > \hbar$ while the sudden quench region sets in for $\tau\Delta_0 < \hbar$.

IV. PHYSICAL REALIZATION

A. Monolayer graphene

The $J=1$ case with $c_1 = v_F \approx 10^6$ m/s is realized in MLG,[25] where the spinor structure encodes the two sublattices of the honeycomb lattice. The control or even the very existence of a gap there remains an open issue. Dirac fermions with linear band crossing can alternatively be realized in optical lattices,[26] where the on-site energies of different sublattices are under control, allowing for the introduction of a time-dependent mass gap. The quantum-Hall step of Eq. (5) represents the hallmark of a single Dirac cone.

B. Bilayer graphene with screening

The $J=2$ case with $c_2=1/2m$ ($m\approx 0.03m_e$) coincides with the low-energy Hamiltonian of BLG (Ref. 27) for energies below $t_\perp/4$, with $t_\perp\sim 0.3-0.4$ eV the interlayer hopping, and the spinor springs from the two layers. Keeping BLG at charge neutrality by either isolating it from the rest of the world in a perpendicular electric field or by using a dual-gate structure,[3–6,28] a continuous change in the gate voltage results in closing and reopening the gap, as the density imbalance between the layers is inverted. Additionally, it also changes the topological properties of the model as in Eq. (5). However, screening due to electron interactions becomes relevant in this case, and the induced gap is related to the external potential, U_{ext} as[2,29]

$$2\Delta = U_{ext} + \frac{e^2 d\,\delta n}{2A_c\varepsilon_r\varepsilon_0}, \tag{10}$$

where $\delta n=\Sigma_p(n_{1p}-n_{2p})$ is the dimensionless density imbalance between the two layers with n_{ip} the particle density of state p on the ith layer. In equilibrium, to a good approximation, the induced gap is given by[1,2]

$$\Delta = \left[1+\lambda\,\ln\left(\frac{4t_\perp}{|U_{ext}|}\right)\right]^{-1}\frac{U_{ext}}{2}, \tag{11}$$

and the density imbalance reads

$$\delta n = 4\rho_0\Delta\,\ln(|\Delta|/2t_\perp) \tag{12}$$

with $\lambda=e^2 d\rho_0/A_c\varepsilon_r\varepsilon_0\sim 0.1-0.5$ the dimensionless screening strength, $d\approx 3.3$ Å the interlayer distance, ε_0 the permittivity of free space, and $\rho_0=A_c m/2\pi\hbar^2$ the density of states per valley and spin in the limit $\Delta\to 0$. For SiO_2/air interface, $\varepsilon_r\approx 2.5$ ($\varepsilon_r=25$ for NH_3 and $\varepsilon_r=80$ for H_2O), which reduces the effects of screening.

V. NUMERICS

In a quench of a time-dependent external potential in BLG, the induced gap couples the two-level systems [stemming from the 2×2 structure of Eq. (1), labeled by p] via the δn term in Eq. (10). The problem would require the solution of a continuum of coupled differential equations, which is not easy, even approximately. We mention that the case of a single level (only one p mode), in which case $\delta n=n_{1p}-n_{2p}$ in Eq. (10), is known as the nonlinear LZ model,[30] and the resulting dynamics differ qualitatively from the conventional one, possessing nonzero transition probability even in the adiabatic limit for strong nonlinear coupling.

The analysis is simplified considerably by the observation that a single level cannot have a strong impact on the dynamics of the others due to the large number of terms in the sum for δn. Thus, it looks natural to replace the nonlinear term by an average density imbalance, independent of the explicit time dependence of $n_{1p}(t)-n_{2p}(t)$ for a given p, hence decoupling the LZ Hamiltonians for distinct p's.

When U_{ext} changes fully adiabatically, the resulting gap and density imbalance are given by Eqs. (11) and (12), respectively. For slow, nearly adiabatic temporal changes in the potential, only a small fraction of terms in the δn sum is expected to behave truly diabatically (contribution from states nearest to the gap edges). Thus we assume that the gap is still given by Eq. (11), and establish self-consistency by verifying that the resulting density imbalance satisfies Eq. (12). Although the usage of Eq. (11) simplifies the picture, it still differs from the conventional LZ form, i.e., subleading logarithmic terms are inevitably present albeit with a reasonably small prefactor λ. Fortunately, one can invoke the extension of the Kibble-Zurek mechanism for nonlinear quenches to estimate the resulting defect density[16,17] (note the difference between a nonlinear quench on the LZ problem[16,17] and the nonlinear LZ problem[30]). The logarithmic terms in Eq. (11) can be considered as "zeroth" powers, therefore the resulting quench is still "linear," with subleading logarithmic corrections.

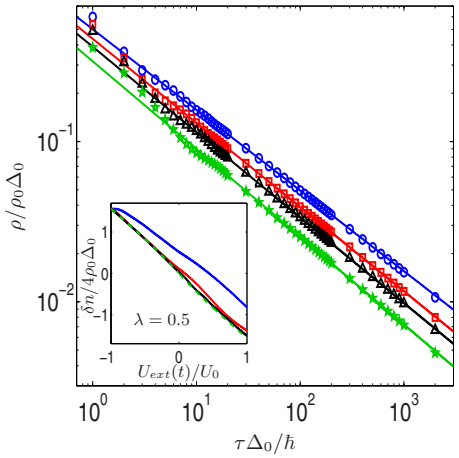

FIG. 2. (Color online) The density of defects created during the quench per spin, valley, and unit cell in BLG with screening is shown for $U_{ext}=U_0 t/\tau$, $t_\perp=5U_0$, $\lambda=0$ (blue, circle), 0.1 (red, square), 0.2 (black, triangle), and 0.5 (green, star) from top to bottom. The symbols denote the numerical data and the solid lines are fits using $\rho/\rho_0\Delta_0=\frac{C}{2}(\frac{\hbar}{\tau\Delta_0})^\alpha$. The inset shows the time-dependent density imbalance of BLG per spin and valley in a linear external potential with strong screening ($\lambda=0.5$) with $\tau\Delta_0/\hbar=1$ (blue), 10 (red), and 100 (black) from top to bottom. The green dashed line shows the fully adiabatic (equilibrium) result with $\tau\to\infty$, Eqs. (11) and (12), which is approached fast with increasing τ. Given the simplicity of our self-consistent average field procedure, the agreement is excellent for slow quenches.

The inset of Fig. 2 shows the density imbalance, obtained from solving numerically the LZ problem [Eq. (7)] with the adiabatic screening potential [Eq. (11)] for BLG with a linearly varying external potential,

$$U_{ext}(t) = U_0 t/\tau, \quad t\in[-\tau,\tau]. \tag{13}$$

The numerical results are compared to those from Eqs. (11) and (12); the imbalance is rather well described by the equilibrium, fully adiabatic ($\tau\to\infty$) expression (dashed-green line), therefore our decoupling of the coupled nonlinear LZ problem by the adiabatic potential for slow enough quenches with Eq. (11) works satisfactorily. This validates our average

TABLE I. The numerically obtained values of the coefficient, $\sqrt{\Delta_\lambda/\Delta_0}$ and the exponent 1/2 of the defect density from Fig. 2 for $t_\perp = 5U_0$, compared to the values based on Kibble-Zurek scaling and Eq. (11).

λ	0	0.1	0.2	0.5
$\sqrt{\Delta_\lambda/\Delta_0}$ from Eq. (11)	1.00	0.88	0.80	0.64
$\sqrt{\Delta_\lambda/\Delta_0}$ from the fit	1.00	0.87	0.78	0.64
Exponent (α)	0.50	0.52	0.53	0.55

field decoupling procedure. Note that to the density imbalance in Eq. (12) all states up to the cutoff, $t_\perp$, are contributing. On the other hand, defect production occurs at very low energies, close to the touching point of the gapless branches, whose contribution to the imbalance is negligible in the limit of the size of the initial gap, Eq. (11), $\Delta_\lambda \equiv \Delta|_{U_{ext}=U_0} \ll t_\perp$.

The number of defects (excited states in the upper branch) created in an external potential, $U_{ext}(t) = U_0 t/\tau$, $t \in [-\tau, \tau]$, follows Eq. (9) even in the presence of screening as

$$\frac{\rho}{\rho_0 \Delta_0} = \frac{1}{2}\sqrt{\frac{\Delta_\lambda}{\Delta_0}}\sqrt{\frac{\hbar}{\tau\Delta_0}}, \tag{14}$$

where $\Delta_0 = |U_0/2|$ and $\Delta_\lambda \equiv \Delta|_{U_{ext}=U_0}$. Equation (14) together with Eq. (9) are the central results of our Kibble-Zurek analysis. The numerical data fitted with $\rho/\rho_0\Delta_0 = C(\frac{\hbar}{\tau\Delta_0})^\alpha/2$, and both the prefactor C and the exponent α are compared to the expected values, namely, $\sqrt{\Delta_\lambda/\Delta_0}$ for the coefficient and 1/2 for the τ exponent for various values of λ, summarized in Table I, and shown in Fig. 2. The agreement is indeed remarkable, the slight mismatch in the exponent 1/2 being due to the subleading logarithmic terms in Eq. (11) for stronger screening. Since $\Delta_0\rho_0 \sim 10^{-3}$ for $\Delta_0 \sim t_\perp/10$, the resulting density of defects per unit area (including spin and valley) falls into the order of $\sqrt{\hbar/\tau\Delta_0} \times 10^{12}$ cm^{-2}, and can take the value 3×10^9 cm^{-2} for quenching time $\tau \sim 1$ ns, corresponding to a ramping rate $\Delta_0/\tau \sim 10^7$ eV/s. Note that this density corresponds to the electrons/holes in the otherwise empty/occupied upper/lower branch, and does not by itself imply any particular real-space density modulation since these states contribute negligibly to the layer charge imbalance. A moderately slow quench implies $\tau\Delta_0/\hbar \sim 10-100$ with $\Delta_0 \sim t_\perp/10$, translating to $\tau \sim 0.1-1$ ps. Different nonlinear sweep protocols[16–18] lead to similar conclusion: the steeper (more nonadiabatic) the quench, the bigger the defect density produced.

Our results are robust with respect to variations in the band structure, e.g., extra hopping terms or large asymmetry gap. The quadratic spectrum of BLG with $J=2$ changes to linear one ($J=1$) at the vicinity of the Dirac point (~10 K range) due to trigonal warping, which could affect the scaling of the defect density ($1/\sqrt{\tau} \to 1/\tau$) for slow quenches. Excitonic effects can either renormalize the gap in biased BLG or open small gaps in unbiased BLG,[31] which can be overcome by the electric field without affecting our findings.

VI. POPULATION INVERSION, DYNAMIC CONDUCTIVITY

Having established the scaling properties of the defect density in BLG, we turn to the determination of the optical response of the excited state resulting from the quench, whose momentum distribution is given by Eq. (8); The occupation number in the upper and lower branches of the spectrum is, respectively, $f_+(p) = P_p$ and $f_-(p) = 1 - P_p$ due to particle-hole symmetry. For momenta close to the K point, population inversion occurs when $f_+(p) > f_-(p)$, i.e., in the energy range $2\Delta_\lambda < \hbar\omega < 2\Delta_\lambda\sqrt{1 + (\hbar \ln 2)/(\pi\Delta_\lambda\tau)}$, which translates in the near adiabatic limit to

$$2\Delta_\lambda < \hbar\omega < 2\Delta_\lambda + \frac{\hbar \ln 2}{\pi\tau}. \tag{15}$$

The effect of a small ac electric field can be considered using Fermi's golden rule, and the initial dynamic conductivity is related to the rate of optical transitions between the two states with the same momentum, weighted by the probabilities of occupied initial and empty final states, as

$$\Gamma_p(\omega) = \frac{2\pi}{\hbar} M_p^2 \delta(\hbar\omega - 2\sqrt{\Delta_\lambda^2 + \varepsilon^2(p)})[f_-(p) - f_+(p)], \tag{16}$$

where $M_p = |v_x(p)eA|$ is the transition matrix element between the higher and lower energy state, where $v_x(p) = \Psi_+^* \partial H/\partial p_x \Psi_-$ and A the vector potential. Thence, we obtain the dynamic conductivity

$$\sigma(\omega) = \sigma_0 \left[1 - 2\exp\left\{\frac{\pi\tau}{4\hbar\Delta_\lambda}[4\Delta_\lambda^2 - (\hbar\omega)^2]\right\}\right] \times \frac{(\hbar\omega)^2 + 4\Delta_\lambda^2}{(\hbar\omega)^2}\Theta(|\hbar\omega| - 2\Delta_\lambda) \tag{17}$$

with $\sigma_0 = e^2/2\hbar$ the ac conductivity of BLG.[32,33]

Both absorption and stimulated emission are taken into account, and the negativity of the resulting conductivity indicates the dominance of the latter: this indicates a phase coherent response, which is of course essential for a laser. In addition, stimulated emission can also win against spontaneous emission by increasing the intensity of the incoming radiation field. If spontaneous emission dominates (luminescence), the resulting radiation will still be spectrally limited but without phase coherence.

In the frequency range of Eq. (15), the dynamic conductivity is negative due to the population inversion[34] (i.e., the energy injected into the system during the quench is released) as

$$\sigma(\hbar\omega \to 2\Delta_\lambda) \approx -2\sigma_0. \tag{18}$$

The region of negative conductivity shrinks with increasing τ, without influencing the amplitude of $\sigma(\omega)$ precisely at the gap edge. This follows from Eq. (8), implying maximal population inversion at the Dirac point for arbitrary quench time, i.e., $P_{p=0} = 1$. For higher frequencies, $\sigma(\omega)$ is still suppressed with respect to the adiabatic optical response.

The typical lasing frequency lies in the close vicinity of Δ_λ (including the terahertz regime, wavelength on the order of 10 μm), conveniently tunable by perpendicular electric fields.[6] The relaxation times for intraband and interband processes in MLG are estimated as 1 ps and 1–100 ns,[34] respectively, which might be further enhanced in BLG around half filling.[35] Thus, the lasing is expected to survive for quenching times in the picosecond-nanosecond range even in the presence of the above processes. Repeated quenching (such as optical pumping) between Δ and $-\Delta$ is also linked to the Kibble-Zurek theory[36] with similar effects on the population inversion.

The dc conductivity also reveals the effect of the electric field quench. In the presence of a clean gap, excitations, and hence the dc conductivity, are exponentially suppressed at low temperatures. The excited electrons/holes in the upper/lower branch resulting from this quench, can carry a current that is not activated.

VII. CONCLUSIONS

To conclude, by exploiting the tunability of the band gap in BLG by a perpendicular electric field, a finite-rate temporal electric field quench leads to excited-state production, whose distribution is analyzed in terms of Kibble-Zurek scaling, LZ dynamics for nonlinear quenches and is compared to the full numerical solution of the problem with screening corrections, using an adiabatic decoupling procedure. The effect of the quench is manifested in population inversion, and BLG could be used as a coherent source of infrared radiation, and possibly as a laser.

Our results apply to other systems with a quadratic band crossing, e.g., for certain nodal superconductors or cold atoms on Kagome or checkerboard optical lattices[37] at appropriate fillings, described by Eq. (1) with $J=2$ at low energies. The momentum distribution, Eq. (8) and the concomitant scaling of the defect density after closing and reopening the gap would be direct evidence of the quench dynamics. Particularly intriguingly, graphene multilayers with appropriate stackings realize higher-order ($J>2$) band crossings.[38,39]

ACKNOWLEDGMENTS

This work was supported by the Hungarian Scientific Research Funds No. K72613 and No. CNK80991 and by the Bolyai program of the Hungarian Academy of Sciences and by the New Hungary Development Plan Nr. TÁMOP-4.2.1/B-09/1/KMR-2010-0002. E.V.C. acknowledges financial support from the Juan de la Cierva Program (MCI, Spain) and the Estímulo à Investigação Program (Fundação Calouste Gulbenkian, Portugal).

*dora@kapica.phy.bme.hu

[1] E. McCann, Phys. Rev. B **74**, 161403(R) (2006).
[2] E. V. Castro, K. S. Novoselov, S. V. Morozov, N. M. R. Peres, J. M. B. Lopes dos Santos, J. Nilsson, F. Guinea, A. K. Geim, and A. H. Castro Neto, J. Phys.: Condens. Matter **22**, 175503 (2010).
[3] J. B. Oostinga, H. B. Heersche, X. Liu, A. F. Morpurgo, and L. M. K. Vandersypen, Nature Mater. **7**, 151 (2007).
[4] K. F. Mak, C. H. Lui, J. Shan, and T. F. Heinz, Phys. Rev. Lett. **102**, 256405 (2009).
[5] F. Xia, D. B. Farmer, Y.-M. Lin, and P. Avouris, Nano Lett. **10**, 715 (2010).
[6] Y. Zhang, T.-T. Tang, C. Girit, Z. Hao, M. C. Martin, A. Zettl, M. F. Crommie, Y. R. Shen, and F. Wang, Nature (London) **459**, 820 (2009).
[7] T. W. B. Kibble, J. Phys. A **9**, 1387 (1976).
[8] W. H. Zurek, Nature (London) **317**, 505 (1985).
[9] B. Damski, Phys. Rev. Lett. **95**, 035701 (2005).
[10] C. Bäuerle, Y. M. Bunkov, S. N. Fisher, H. Godfrin, and G. R. Pickett, Nature (London) **382**, 332 (1996).
[11] V. M. Ruutu, V. B. Eltsov, A. Gill, T. W. Kibble, M. Krusius, Y. G. Makhlin, B. Placais, G. E. Volovik, and W. Xu, Nature (London) **382**, 334 (1996).
[12] I. Chuang, R. Durrer, N. Turok, and B. Yurke, Science **251**, 1336 (1991).
[13] M. J. Bowick, L. Chandar, E. A. Schiff, and A. M. Srivastava, Science **263**, 943 (1994).
[14] L. E. Sadler, J. M. Higbie, S. R. Leslie, M. Vengalattore, and D. M. Stamper-Kurn, Nature (London) **443**, 312 (2006).
[15] W. H. Zurek, U. Dorner, and P. Zoller, Phys. Rev. Lett. **95**, 105701 (2005).
[16] R. Barankov and A. Polkovnikov, Phys. Rev. Lett. **101**, 076801 (2008).
[17] D. Sen, K. Sengupta, and S. Mondal, Phys. Rev. Lett. **101**, 016806 (2008).
[18] C. De Grandi, V. Gritsev, and A. Polkovnikov, Phys. Rev. B **81**, 012303 (2010).
[19] M. V. Berry, Proc. R. Soc. London, Ser. A **392**, 45 (1984).
[20] D. J. Thouless, M. Kohmoto, M. P. Nightingale, and M. den Nijs, Phys. Rev. Lett. **49**, 405 (1982).
[21] J. E. Avron, D. Osadchy, and R. Seiler, Phys. Today **56**(8), 38 (2003).
[22] M. Uhlmann, R. Schützhold, and U. R. Fischer, Phys. Rev. D **81**, 025017 (2010).
[23] N. V. Vitanov and B. M. Garraway, Phys. Rev. A **53**, 4288 (1996).
[24] J. Dziarmaga, Phys. Rev. Lett. **95**, 245701 (2005).
[25] A. H. Castro Neto, F. Guinea, N. M. R. Peres, K. S. Novoselov, and A. K. Geim, Rev. Mod. Phys. **81**, 109 (2009).
[26] A. Dutta, R. R. P. Singh, and U. Divakaran, EPL **89**, 67001 (2010).
[27] E. McCann and V. I. Fal'ko, Phys. Rev. Lett. **96**, 086805 (2006).
[28] S. Kim and E. Tutuc, arXiv:0909.2288 (unpublished).
[29] H. Min, B. Sahu, S. K. Banerjee, and A. H. MacDonald, Phys. Rev. B **75**, 155115 (2007).
[30] B. Wu and Q. Niu, Phys. Rev. A **61**, 023402 (2000).
[31] R. Nandkishore and L. Levitov, arXiv:1002.1966 (unpublished).
[32] D. S. L. Abergel and V. I. Fal'ko, Phys. Rev. B **75**, 155430

(2007).
[33] E. J. Nicol and J. P. Carbotte, Phys. Rev. B **77**, 155409 (2008).
[34] V. Ryzhii, M. Ryzhii, and T. Otsuji, J. Appl. Phys. **101**, 083114 (2007).
[35] M. Monteverde, C. Ojeda-Aristizabal, R. Weil, K. Bennaceur, M. Ferrier, S. Gueron, C. Glattli, H. Bouchiat, J. N. Fuchs, and D. L. Maslov, Phys. Rev. Lett. **104**, 126801 (2010).
[36] V. Mukherjee, A. Dutta, and D. Sen, Phys. Rev. B **77**, 214427 (2008).
[37] K. Sun, H. Yao, E. Fradkin, and S. A. Kivelson, Phys. Rev. Lett. **103**, 046811 (2009).
[38] F. Guinea, A. H. Castro Neto, and N. M. R. Peres, Phys. Rev. B **73**, 245426 (2006).
[39] H. Min and A. H. MacDonald, Phys. Rev. B **77**, 155416 (2008).